NMR Studies of Carbosilane Dendrimer with Terminal Mesogenic Groups

Denis A. Markelov,*,†,‡,§ Vladimir V. Matveev,‡ Petri Ingman,|| Marianna N. Nikolaeva,§ Erkki Lähderanta,† Vladimir A. Shevelev,§ and Natalia I. Boiko⊥

Laboratory of Physics, Lappeenranta University of Technology, Box 20, 53851 Lappeenranta, Finland, Faculty of Physics, St. Petersburg State University, Ulyanovskaya Str. 1, Petrodvorets, St. Petersburg, 198504 Russia, Institute of Macromolecular Compounds, Russian Academy of Sciences, Bolshoi Prospect 31, V.O., St. Petersburg, 199004 Russia, Instrument Centre, Department of Chemistry, University of Turku, Vatselankatu 2, FI-20014, Turku, Finland, and Faculty of Chemistry, Moscow State University, eninskie gory, Moscow, 119991 Russia

Received: October 8, 2009; Revised Manuscript Received: February 2, 2010

The 4-generation carbosilane dendrimer with terminal cyanobiphenyl mesogenic groups in dilute solution of $CDCl_3$ was investigated using ^1H NMR technique. The spectrum was obtained and the relaxation time, T_1, was measured in the temperature range 320−225 K. For the first time, the extrema of T_1 values were achieved for majority of the dendrimer functional groups. The values of activation energies of the dendrimer functional groups were obtained. The relaxation data for outer and inner methyl groups show that the dendrimer investigated has dense corona and hollow core. This structure is formed because the mesogenic groups do not allow terminal segments to penetrate into the dendrimer, that is, the backfolding effect is absent. The NMR spectral and relaxation data give evidence for changing conformation of the dendrimer internal segments with decreasing temperature. This reorganization is most likely connected with a change of dendrimer size. We suppose that our experimental results will provide additional information for understanding principles of dendrimer nanocontainer operation. NMR can possibly be a tool for indicating the encapsulation effect as well as the dendrimer effective size.

1. Introduction

Dendrimers, being a relatively new kind of polymer system possessing a number of unique characteristics, are used in different areas of polymer chemistry, biology, and medicine.[1] In many cases, practical application of a dendrimer is determined by its molecular mobility. The dendrimer mobility is studied by various methods, such as dielectric relaxation, polarized luminescence, double refraction, NMR, and so forth.[2−31]

The use of dendrimers as nanocontainers for anticancer drugs, dyes, and metal nanoparticles is of particular interest (see, for example, refs 2−9). This is possible due to the attachment or sorption of substances on dendrimer terminal groups and dendrimer ability to encapsulate substances in dilute solution. As a rule, dendrimers used for encapsulation possess dense superficial layer (corona) and relatively hollow core.[31] Experimental data[10−12,14] and computer simulation methods[13] show that this structure can be realized, particularly, in generation-4 carbosilane dendrimers (CSD) with terminal mesogenic groups. It was shown[10−13] that mesogenic groups are localized on the surface of the molecule and do not penetrate into dendrimer, that is, there is no backfolding. Also, the generation-4 CSD has spherical form in dilute solution.[14] These facts allow one to assume that CSD molecules have dense superficial layer (corona) and hollow core if the spacer between mesogenic groups and the dendrimer is short.

* To whom correspondence should be addressed. E-mail: markeloved@gmail.com.
† Lappeenranta University of Technology.
‡ St. Petersburg State University.
§ Russian Academy of Sciences.
|| University of Turku.
⊥ Moscow State University.

NMR is one of the most effective methods of studying different polymer systems.[32] For instance, it is used in investigating structure and dynamic properties of dendrimers.[15−23,28−30,33−37] Methods of obtaining NMR spectra and measuring diffusion parameters are well developed; self-diffusion was studied for a number of dendrimers in solutions over a wide range of sample concentrations by NMR technique.[19,28−30] In particular, it was shown that the generalized dependence of the self-diffusion coefficient of CSDs coincides with the analogous dependence for globular protein in aqueous solutions.[28,29]

One of the most informative methods of studying local mobility of macromolecules is the spin−lattice relaxation, T_1. However, this experimental technique is poorly applied for studies of local mobility inside dendrimers and is mostly used as an additional tool for qualitative analysis.[33,34] On the other hand, the T_1 relaxation analysis was carried out in detail for different terminal groups of dendrimers.[17,22,23,32,36,37] In particular, melt of CSD with terminal mesogenic groups was investigated by NMR technique in liquid crystalline phase.[17,22,23] In this case, the dendrimer was used as a matrix that creates higher local concentration of mesogenic groups.

In recent works,[38,39] orientational mobility of dendrimer segments was studied using Brownian dynamics simulation. As was shown,[39] the theory of spin−lattice relaxation T_1 near extremum is determined by relaxation process which corresponds to local reorientation of an individual segment in dendrimer. More large-scale processes, such as the rotation of a dendrimer branch (pulsation) and the dendrimer rotation as a whole, do not influence the T_1 trend. It is important to note that the local reorientation is determined by the minimal relaxation time which does not practically depend on the location of the segment.[39−41] This fact gives one reason to fit the T_1 trend in the range of extremum by one-time approximation.

10.1021/jp909658v
Published on Web 03/04/2010

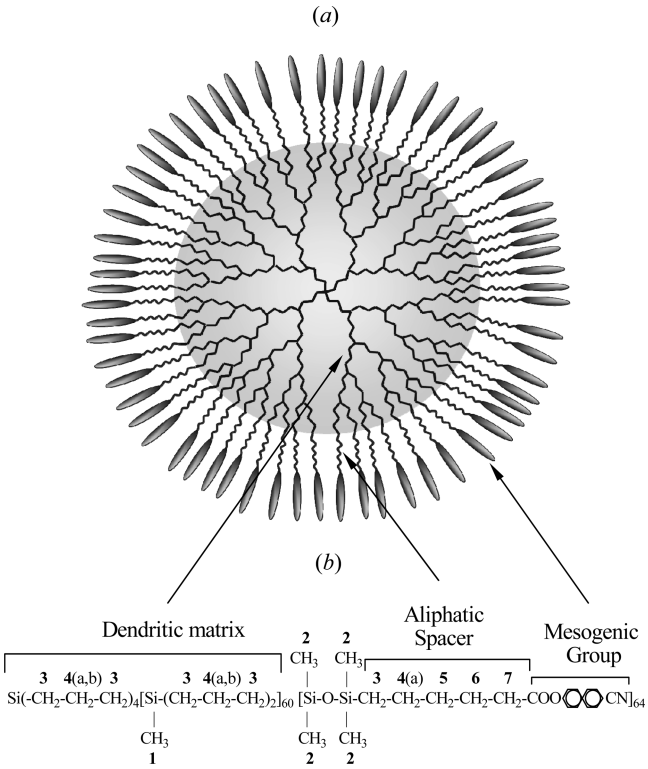

Figure 1. Schematic (a) and structural (b) formulas of the 4-generation carbosilane dendrimer with terminal cyanobiphenyl mesogenic groups. Numbers 1−7 refer to Figure 2 and Table 1.

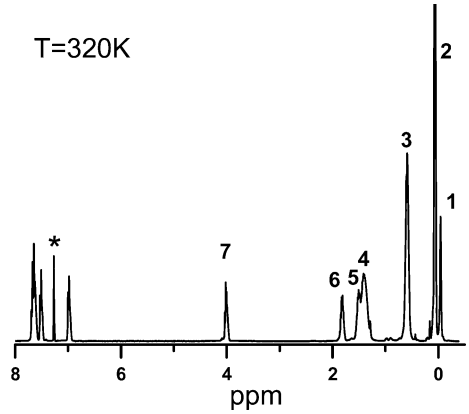

Figure 2. ^{1}H NMR spectrum of the 4-generation carbosilane dendrimer at 320 K. The spectrum is calibrated by chloroform peak (*) at 7.25 ppm. The attribution of peaks (1−7) is shown in Figure 1 and Table 1.

The present work is devoted to the NMR study of conformational and dynamical properties of CSD in solution. We studied the dilute solution of 4-generation CSD with terminal cyanobiphenyl mesogenic groups linked by $-(CH_2)_5-$ short aliphatic spacer (AS). The temperature dependencies of the dendrimer NMR spectra and relaxation time T_1 were analyzed. The structural formula of the studied compound is shown in Figure 1. The rest of the paper is organized as follows. Experimental details are described in Section 2. In Section 3, the ^{1}H NMR spectra and the temperature dependencies of NMR relaxation rates for different spectral lines are described. In Section 4, short summary and conclusions are given.

2. Experimental Section

The synthesis of the dendrimer studied was described earlier.[24,25] The sample (CSD with terminal cyanobiphenyl groups) was solved in deuterochloroform $CDCl_3$ (concentration 2−3 wt %). The measurements were carried out at 400 MHz using a BRUKER AVANCE 400 spectrometer. No deuterium lock was used; the remanent proton signal of $CDCl_3$ with chemical shift (δ) 7.25 ppm was used as an internal reference for δ calculation of other spectral lines. No temperature dependence correction was made for the δ ($CDCl_3$).

TABLE 1: Identification of ^{1}H NMR Spectrum Peaks with Dendrimer Functional Groups and Aliphatic Spacer[a]

type of group	CH_3		CH_2				
peak number in spectrum	1	2	3	4	5	6	7
δ (ppm)	−0.08	0.02	0.55	1.37	1.48	1.79	3.98
peak integrals[b]	1.41	6.01	4.68	3.06	1.13	1.03	1.00
number of groups in the sample[b]	0.937	4	4.875	2.94	1	1	1
neighbors	Si	Si	Si CH_2	CH_2 CH_2	CH_2 CH_2	CH_2 CH_2	CH_2 COO

[a] The number of functional groups was calculated using peak integral values. Calculation was made at T = 320 K. [b] Peak integrals and the number of groups were normalized using the parameters of peak 7.

The proton spin−lattice relaxation times, T_{1H}, were measured using conventional inversion−recovery $\pi-\tau-\pi/2$ pulse sequence with 6 μs duration of $\pi/2$ pulse, 14 scans for each T_{1H} measurement, and a 6.3 s recycle delay time between scans. This was much longer than any measured $5T_{1H}$. The T_{1H} values were extracted using the expression

$$\frac{M(t)}{M_0} = [1 - k\exp(t/T_{1H})] \quad (1)$$

where M_0 and $M(t)$ are the magnetization at equilibrium and at time t, respectively. M_0, k, and T_{1H} were calculated as free parameters using the least-mean-square method. Ideally, the k should be equal to 2, but for all experiments, the obtained k values were between 1.7 and 2.0.

Temperature range (320−225 K) was limited by the boiling and freezing points of deuterochloroform.

3. Results and Discussion

3.1. NMR Spectrum. ^{1}H NMR spectrum of the investigated CSD is shown in Figure 2. An analogous dendrimer was studied earlier[24] with the full attribution of the spectrum peaks. Using these results and relative integral intensities of the spectral lines, we can assign the most part of the peaks to structural groups of the investigated dendrimer (see Table 1 and Figures 1 and 2). Peaks 1 and 2 correspond to inner and outer CH_3-groups (Figure 1b), respectively. Hereafter, the groups of the dendrimer itself are referred to as inner groups, and the ones in AS and in the junction connecting AS with a dendrimer are referred to as outer groups (see Figure 1b). Peak 3 is related to $-CH_2-Si$ protons, including protons in inner CSD groups (79%) and the spacer ones (21%).

Peaks 4−7 were assigned to the rest of CH_2-groups of CSD and AS. Identification of peaks 7 and 6 as signals of AS methylene groups, which are the nearest neighbors to COO-group (accordingly α- and β-), presents no difficulties and is analogous to the one in ref 24. Peaks 4 and 5, however, required more detailed consideration. Peak 5 is attributed to the spacer γ-CH_2 group. We were able to observe a signal of this group due to higher spectrometer frequency as compared to the one

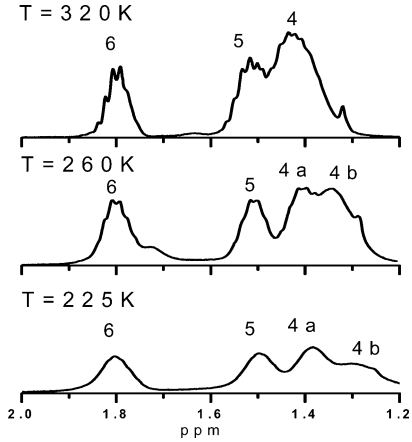

Figure 3. Evolution of peaks 4−6 of ^{1}H NMR spectrum of the 4-generation carbosilane dendrimer with changing temperature. Identification of peaks is given in Figure 1 and Table 1.

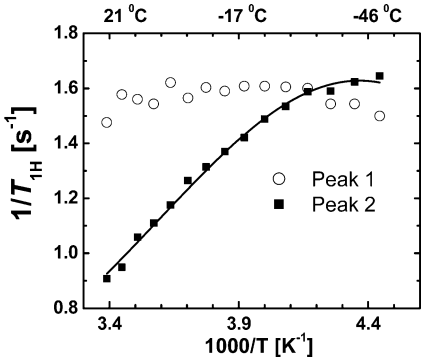

Figure 4. Temperature dependence of ^{1}H NMR relaxation rate of inner (circles) and outer (squares) CH_3-groups. Solid line shows fit by eqs 2−4.

in ref 24. Similarly to ref 24, peak 4 includes signals of AS methylene groups (34%) and CSD ones (66%). As this line is a superposition of two signals (4a and 4b), its shape depends on temperature (see Figure 3). It is important for further consideration that the integrals of peaks 3, 4, and 5 are in correct ratios with the integrals of peaks 6 and 7 (Table 1) and that all observed peaks in our spectrum, including 4a and 4b, do not practically change their positions with decreasing temperature.

Signals located to the left of peak 7 can be attributed to the CH− bonds of the mesogenic groups[22,24] and will not be considered further.

3.2. Temperature Dependence of NMR Relaxation Times. The measured relaxation times, T_{1H}, for all spectral lines are shown in Figures 4−6 as a function of temperature. ^{1}H NMR relaxation time is determined by the well-known equation (e.g., see ref 42)

$$\frac{1}{T_{1H}}(\omega_0, T) = A_0(J(\omega_0, T) + 4J(2\omega_0, T)) \qquad (2)$$

where ω_0 is the Larmor frequency, T is the temperature, $A_0 = 3\gamma^4\hbar^2/10r_0^6$ is the dipolar coupling constant, γ is the gyromagnetic ratio for ^{1}H nuclei; r_o is the effective ^{1}H−^{1}H distance, and $J(\omega_0,T)$ is the spectral density function. For the cases observed this function can be written in its simplest form

$$J(\omega_0, T) = \frac{\tau_{cor}(T)}{1 + (\omega_0\tau_{cor}(T))^2} \qquad (3)$$

where τ_{cor} is the correlation time controlling $1/T_{1H}$ temperature dependence. Since dendrimer macromolecules possess the specific relaxation spectrum,[43−47] orientational segmental mobility is determined by three relaxation processes.[38,39,48] They are (i) the rotation of the dendrimer as a whole with the characteristic time τ_{rot}, (ii) the rotation of the dendrimer branch originating from a given segment with the relaxation time τ_{br}, and (iii) the local reorientation of the segment with the average time of the dendrimer internal spectrum, τ_{in}. It was shown[39] that the τ_{cor} in eq 3 is controlled mainly by mobility of the segment reorientation due to the fact that $\tau_{in} \ll \tau_{br} < \tau_{rot}$ and by ratios between the relaxation processes. The large-scale motions, such as the dendrimer branches pulsation and the dendrimer rotation as a whole, do not practically influence the $1/T_{1H}$ maximum.

It is important to mention that a segment in this case is modeled by a rigid rod. There is a typical way for computer simulation studying dynamic properties of polymer systems. The results of these model simulations have good agreement for dendrimers with different structures, for example, see refs 32, 40, and 41. These data indicate that the total relaxation T_1 of all dendrimer segments for the same functional groups of the segment is determined by the same relaxation time. This is because τ_{in} practically does not depend on the location of a dendrimer segment.[38−41,48] Although CSDs with modified terminal segments are considered, we suppose that the use of the simple form of $J(\omega_0,T)$ is quite possible.

In the simplest way, the temperature dependence of the correlation time is described by the Arrhenius function

$$\tau_{cor}(T) = \tau_0 \exp(E_a/k_BT) \qquad (4)$$

where E_a is the activation energy for the chosen group.

Before we proceed to consideration of the relaxation dependences (Figures 4−6), it is necessary to point out that we could achieve the maximum of $1/T_{1H}$, the so-called "dispersion range", for practically all spectral lines. To the best of our knowledge, this is the first observation of the NMR dispersion range in dendrimer solutions. This range was not reached for PAMAM dendrimer in aqueous solution[18] because of water freezing. A minimum of spin−spin relaxation time, T_2, observed for a melt of similar CSD samples,[22,34,37] was connected to the isotropic liquid−liquid crystal macrophase transition. The dispersion range in dendrimer was observed also in magnetic resonance imaging studies.[49−52] However, as a rule, T_{1H} signal for all hydrogen-containing groups was measured. In this case, eq 3 cannot be used because different functional groups, for example CH_2 and CH_3, have different correlation times.

It is well-known from the theory of NMR relaxation and obvious from eqs 2−4 that the dispersion range allows direct calculation of τ_{cor} for each functional group of the compound (in our case, of the dendrimer). This calculation was made; the results are shown in Table 2. However, we will start the discussion from the description of some trends in temperature dependence of the behavior of dendrimer functional groups, as the practically complete assignment of spectrum peaks was made.

3.2.A. Methyl Groups. The temperature dependence of relaxation rate for inner methyl groups differs strongly from all other lines, including that of outer CH_3 groups (Figure 4);

TABLE 2: Calculations of Mobility Parameters in Equations 2−4[a]

peak number	$A_0\ 10^{-10}$ (±20%)	τ_0 [ps] (±20%)	E_a [kJ/mol] (±4%)	T_{max}, [K] (±3 K)	τ_{cor}, [ns] for $T = 273$ K
2	0.29	0.99	10.48/9.81	229	0.10
3[b]	0.40	0.95	12.19	265	0.20
4b[b]	0.43	1.11	11.99	267	0.22
4a	0.48	0.43	12.69	241	0.12
5	0.55	0.21	13.99/10.23	238	0.10
7	0.57	0.33	12.98/11.89	236	0.10

[a] E_a is the activation energy (full fit/Arrhenius fit) and T_{max} is the temperature of $1/T_{1H}$ maximum. [b] For peaks 3 and 4b low temperatures (225−240 K) were not taken into account in the fit of temperature dependence of $1/T_{1H}$ near maximum. In this case, the location of maximum of fit results coincided with experimental data.

specifically, the relaxation rate is virtually independent of temperature. According to eqs 2−4, it corresponds to near zeroth E_a value and means that inner methyl groups have practically free rotation. In this case, the question of whether we reached the dispersion range for inner methyl groups or not remains open. On the other hand, such behavior allows us to conclude that there is enough free space in the vicinity of the group, that is, this fact unambiguously indicates that the dendrimer has sufficiently hollow core structure.

On the contrary, $1/T_{1H}$ of outer methyl groups shows visible temperature dependence (Figure 4). Unfortunately, we could not achieve the clear maximum of this dependence in the temperature range used. Nevertheless, experimental data allow us to calculate E_a using both standard fit (according to eqs 2−4) and low temperature approximation (Arrhenius plot) when the so-called "extreme narrowing" conditions ($\omega_0\tau_{cor} \ll 1$) are valid. Both fits give close E_a values (Table 2), and it means that we could obtain correct value of activation energy for the outer CH_3 groups in the temperature region concerned.

On the other hand, this E_a of methyl groups significantly (~10 kJ/mol) exceeds the expected activation energy values for the solutions of polymers with similar chemical structure. For example, E_a for polydimethylsiloxanes in solution is less than 8 kJ/mol.[53] We suppose that the increase of E_a in our solution is caused by the dense corona that is formed due to the short AS and location of terminal mesogenic groups on the surface of the CSD.

Comparison of these results gives an extra evidence for the presence of sufficiently hollow core and relatively dense terminal shell in the dendrimer. If our conclusion is true, temperature dependence of T_{1H} of inner methyl groups can be used as an indicator of CSD with hollow core.

3.2.B. Methylene Groups. Temperature dependences of $1/T_{1H}$ for methylene groups of AS (peaks 5 and 7) show almost similar behavior; the temperatures at which $1/T_{1H}$ maximum is observed (T_{max}) are practically equal (Figure 5). Fitting these data by eqs 2−4 leads to the results summarized in Table 2. E_a values obtained from the full fit are higher than E_a calculated from Arrhenius approximation. It means that $\omega_0\tau_{cor} \ll 1$ condition is not valid for peaks 5 and 7 even at the highest temperatures reached in our experiments.

In contrast to the facts stated above, the temperature dependence measured for peak 3 shows higher T_{max} (Figure 6), and both parts of the curve are observed. As the major contribution (79%) to peak 3 is made by the CSD methylene groups (inner methylene groups), it means that T_{max} for these groups is higher as compared to AS methylene ones. Unfortunately, it turned out impossible to use all experimental points

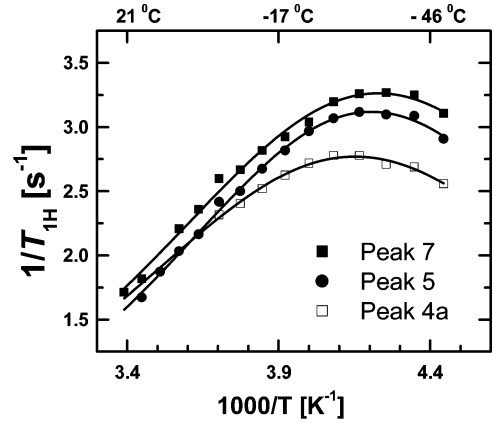

Figure 5. Temperature dependence of ^{1}H NMR relaxation rate of aliphatic spacer CH_2 groups. Solid line shows fit by eqs 2−4.

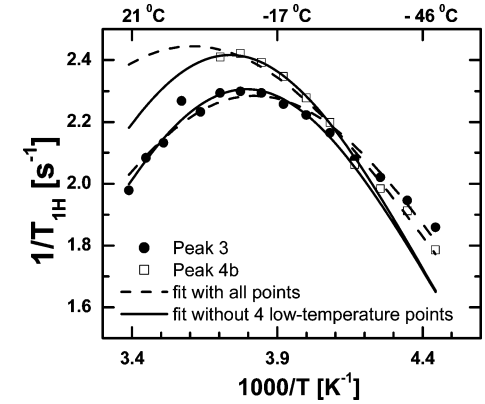

Figure 6. Temperature dependence of ^{1}H NMR relaxation of carbosilane dendrimer CH_2 groups for peaks 3 and 4. Solid and dashed lines shows fit by eqs 2−4. No Arrhenius fit for this peak was made.

to fit the dependence, and it looks evidently asymmetric as opposed to eqs 2−4. One reason of the asymmetry is an increasing contribution of AS methylene groups in the low-temperature part of the dependence. These groups account for 21% of peak 3, and their $1/T_{1H}$ value reaches maximum just in this temperature range (see Figure 5). Therefore, we excluded the last three low-temperature points from the fitting procedure, and the parameters obtained are given in Table 2.

Since peaks 4a and 4b were resolved in the majority of cases, we succeeded in measuring their relaxation rates separately, and the dependences were significantly different. Figure 5 shows that for peak 4a the $1/T_{1H}$ behavior practically coincides with relaxation of outer CH_2 groups belonging to AS (peak 5 and 7). Concerning the relaxation rate of peak 4b, it looks more complicated. No separate peak 4b was observed above 270 K, and experimental points available lie at $T < \sim T_{max}$. As follows from the experimental points (Figure 6), the position of the maximum is close to the T_{max} of inner groups (peak 3). On the other hand, the fit with all experimental points shown by the dot line in Figure 6 led to significantly higher T_{max}, which did not correspond to any group in the dendrimer. Apparently, relaxation of the low-temperature points was again strongly affected by the contribution of AS methylene groups similar to peak 3. Indeed, exclusion of two low-temperature points from the fitting procedure led to satisfactory agreement with the experiment; the corresponding fit curve is shown in Figure 6 by solid line.

TABLE 3: Intensity Ratio, I_{4b}/I_{4a}, and the Conformational Probability Ratio, p_b/p_a, for Peaks 4a and 4b at Different Temperatures[a]

T (K)	I_{4b}/I_{4a}	p_b/p_a
320	0	0
260	1	3
225	1.5	9

[a] p_b/p_a corresponds only to inner CSD segment.

Thus, the experimental data showed that the relaxation peak 4a corresponds mainly to AS methylene groups and the peak 4b to the dendrimer inner methylene groups (see Figure 1b).

In this connection, we should consider splitting of peak 4 in more detail using both spectral and relaxation data. As mentioned earlier, the shape of line 4 is changing considerably with decreasing temperature (Figure 3). The single peak is observed at 320 K, and at lower temperatures the signal splits to peaks 4a and 4b. The behavior of peak 4 has two significant features. First, in the temperature range from 260 to 225 K chemical shifts of peaks 4a and 4b practically do not change. It means that the line splitting is not a result of dynamic NMR, that is, of spectrum transformation between "fast exchange" and "slow exchange" regimes. On the contrary, the line splitting looks like a result of the population redistribution of the methylene groups between two different conformations with more or less fixed chemical shifts.

Second, the integral intensity ratio, I_{4b}/I_{4a}, increases as the temperature decreases (Table 3). It confirms that peaks 4a and 4b do not correspond to different groups of CSD and/or AS but reflect different conformational states of the same groups.

Thus, at higher temperature the majority of central methylene groups of either AS or CSD have the same conformation. This conformation corresponds to peak 4a, as no peak 4b is observed in Figure 2 or 3. With decreasing temperature some of methylene groups transit to other conformational state, which can be identified with peak 4b (Table 3). The $1/T_{1H}$ temperature dependence allows one to conclude that peak 4b mainly corresponds to the inner methylene groups at least for temperatures $\leq$260 K (Figures 5 and 6). It is reasonable to suppose that only inner CSD segments transit into another conformational state. This assumption is confirmed by the fact that peaks 5−7 assigned to AS methylene groups do not split with decreasing temperature. On the other hand, peak 3 corresponding to inner methylene groups does not change its shape. This phenomemon can be explained by the fact that the methylene groups of peak 3 have Si atom as a neighbor. Most of Si atoms are branching points. Hence, the NMR relaxation depends on two conformations corresponding to two branches. The T_1 correlation time is determined by the conformation which decelerates mobility of the methylene groups.

The inner segment connected with dendrimer branching points can exist in two conformational states with different segment lengths,[54] namely the "stretched" trans-conformation and the "curled" gauche-conformation (Figures 7a and 7b). To describe this situation, we have used the common two-state segment model[55−57] when two conformational states (trans- and gauche-) having different segment lengths are separated by an internal rotation barrier (Figure 7c).

Our experimental data do not allow the determination of the conformational state of CSD segments at low or high temperatures independently. Relying on the recent data,[54] we suppose that at high temperature both CSD and AS segments have trans-conformation, that is, peak 4a corresponds to trans-conformation and peak 4b corresponds to gauche-conformation. The distribution of populations between gauche- and trans- conformations can be described by common Boltzmann's factor

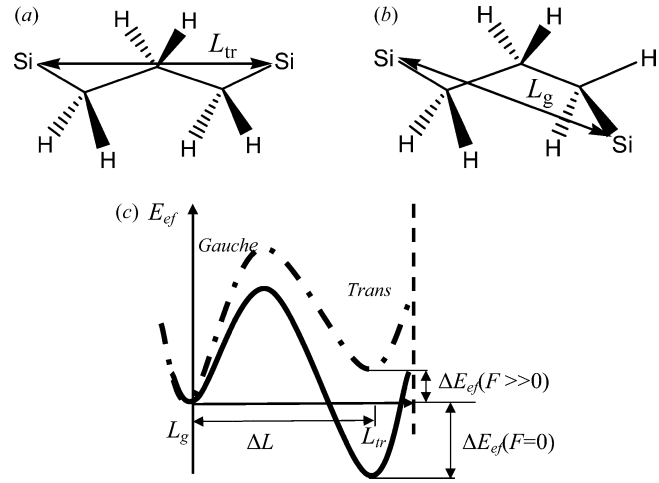

Figure 7. Trans- (a) and gauche-(b) conformational states of the inner segment of the dendrimer with the scheme of effective potential energy barrier (c) separating these conformational states (gauche- and trans-). L_g and L_{tr} are the segment lengths of gauche- and trans-conformers, respectively, $\Delta L = L_{tr} - L_g$ is the segment length difference, $\Delta E_{ef}(F)$ is the energy difference of gauche- and trans-conformers, F is the effective force applied to segment ends.

$$p_b/p_a = \exp\left(\frac{\Delta E_{ef}}{k_B T}\right) \quad (5)$$

where p_a and p_b are the population probabilities of trans- and gauche-conformations, respectively, $\Delta E_{ef} = E_b - E_a$ is the energy difference between the states, and E_b and E_a are the effective energies of these states. To estimate the p_b/p_a value, we neglected the fact that small part of AS segments in the low-temperature region has gauche-conformation and contributes to the peak 4b. Then, p_b/p_a depends on intensities I_{4a} and I_{4b}, which can be expressed as follows

$$p_b/p_a \approx \frac{I_{4b}}{\frac{N_{CSD}}{N_{CSD}+N_{AS}}(I_{4a}+I_{4b})} \approx \frac{I_{4b}}{\frac{2}{3}(I_{4a}+I_{4b})} \quad (6)$$

Here N_{CSD} and N_{AS} are the amounts of the methylene groups corresponding to CSD and AS, respectively, and $N_{CSD}(I_{4a}+I_{4b})/(N_{CSD}+N_{AS})$ is the contribution of the inner segments to the intensity of peak 4 according to the structural formula of CSD shown in Figure 1b. The results of calculation of p_b/p_a for some defined temperatures are given in Table 3. If ΔE_{ef} in eq 5 does not depend on T, $p_a/p_b \rightarrow 1$ in high-temperature limit and $p_a/p_b \rightarrow 0$ or $+\infty$ in low-temperature one, depending on the sign of ΔE_{ef}. However, this prediction is in contrast with our experimental results (Table 3), because $p_b/p_a \rightarrow 0$ with increasing temperature. To describe this effect, it is necessary to take into account the sign of ΔE_{ef} and especially possible dependence of ΔE_{ef} on the effective constringent force, F, applied to the segment ends[55−57]

$$\Delta E_{ef}(F) = \Delta E_{ef}(F=0) + F\Delta L \quad (7)$$

where ΔL is the length difference of the conformational states. In the absence of forces, segments of CSD and AS commonly have trans-conformation, that is, $\Delta E_{ef}(F = 0) < 0$. However, with growing F value, ΔE_{ef} may increase and become positive leading to gauche-conformation of the segments (see Figure 7c). This approach can describe the observed reorganization effect of the conformation.

It is interesting to discuss the origin of F in eq 7. Typically, generation-4 CSD has a spherical form.[14] Also, as was mentioned above, our NMR relaxation data show that the investigated CSD sample with mesogenic groups has sufficiently dense corona and relatively hollow core. This structure leads to an additional tension force inside the dendrimer. The change of this force with decreasing temperature is most likely caused by the change of dendrimer size. However, it is clear that the conformation changing probably corresponds to the change of CSD sample. Size control can be very important for studies of encapsulation effect; we suppose that additional experiments and computer simulations will help to reveal the cause of size change.

4. Summary

In the present work, the 4-generation carbosilane dendrimer with terminal cyanobiphenyl mesogenic groups in dilute solution of deuterochloroform has been studied by ^{1}H NMR technique. The spectrum and the relaxation time T_1 were obtained within the temperature range from 320 to 225 K.

We have found NMR relaxation rate maxima for all functional groups of the dendrimer solution investigated and measured directly the corresponding characteristic times for internal rotation of these groups.

The comparison of outer and inner methyl groups indicates that CSD possesses hollow core and relatively dense terminal shell. The temperature dependence of T_{1H} of inner methyl groups can be used as an indicator of the presence of hollow core in CSD.

We have for the first time detected the splitting of the line of internal methylene groups into two peaks. We attribute the unusual temperature dependence of the line shape to the inner segment transformation between gauche- and trans-conformers. This reorganization is most likely connected with the change of CSD size.

In summary, both spectral and relaxation experimental results lead to conclusion that the investigated dendrimer (i) possesses dense corona and hollow core and (ii) can change its size with temperature decrease.

Acknowledgment. This work was supported by the Russian Foundation for Basic Research (Grants 08-03-01139 and No. 08-03-00150).

References and Notes

(1) Frechet, J. M. J.; Tomalia, D. A. *Dendrimers and Other Dendritric Polymers*; Wiley: New York, 2002.
(2) Kono, K.; Miyoshi, T.; Haba, Y.; Murakami, E.; Kojima, C.; Harada, A. *J. Am. Chem. Soc.* **2007**, *129*, 7222–7223.
(3) Bernhardt, S.; Kastler, M.; Enkelmann, V.; Baumgarten, M.; Mullen, K. *Chem.—Eur. J.* **2006**, *12*, 6117–6128.
(4) Dhanikula, R. S.; Hildgen, P. *Bioconjugate Chem.* **2006**, *17*, 29–41.
(5) Demadis, K. D. *J. Chem. Technol. Biotechnol.* **2005**, *80*, 630–640.
(6) Fernandez, G.; Sanchez, L.; Perez, E. M.; Martın, N. *J. Am. Chem. Soc.* **2008**, *130*, 10674–10683.
(7) Calabretta, M. K.; Kumar, A.; McDermott, A. M.; Cai, C. *Biomacromolecules* **2007**, *8*, 1807–1811.
(8) Patri, A. K.; Majoros, I. J.; Baker, J. R. *Curr. Opin. Chem. Bio.* **2002**, *6*, 466–471.
(9) Majoros, I. J.; Myc, A.; Thomas, T.; Mehta, C. B.; Baker, J. R. *Biomacromolecules* **2006**, *7*, 572–579.
(10) Lezov, A. V.; Mel'nikov, A. B.; Polushina, G. E.; Antonov, E. A.; Novitskaya, M. E.; Boiko, N. I.; Ponomarenko, S. A.; Rebrov, E. A.; Shibaev, V. P.; Ryumtsev, E. I.; Muzafarov, A. M. *Dokl. Akad. Nauk* **2001**, *381*, 313–316.
(11) Lezov, A. V.; Polushina, G. E.; Mikhailova, M. E.; Rebrov, E. A.; Muzafarov, A. M.; Ryumtsev, E. I. *Russ. J. Phys. Chem.* **2003**, *77*, 944–947.
(12) Kovshik, A. P.; Ragimov, D. A.; Kovshik, S. A.; Boiko, N. I.; Lezov, A. V.; Ryumtsev, E. I. *Russ. J. Phys. Chem.* **2003**, *77*, 935–939.
(13) Wilson, M. R.; Ilnytskyi, J. M.; Stimson, L. M. *J. Chem. Phys.* **2003**, *119*, 3509–3515.
(14) Stark, B.; Lach, C.; Farago, B.; Frey, H.; Schlenk, C.; Stuhn, B. *Colloid Polym. Sci.* **2003**, *281*, 593–600.
(15) Meltzer, A. D.; Tirrell, D. A.; Jones, A. A.; Inglefield, P. T.; Hedstrand, D. M.; Tomalia, D. A. *Macromolecules* **1992**, *25*, 4541–4548.
(16) Meltzer, A. D.; Tirrell, D. A.; Jones, A. A.; Inglefield, P. T. *Macromolecules* **1992**, *25*, 4549–4552.
(17) Ponomarenko, S. A.; Boiko, N. I.; Shibaev, V. P.; Richardson, R. M.; Whitehouse, I. J.; Rebrov, E. A.; Muzafarov, A. M. *Macromolecules* **2000**, *33*, 5549–5558.
(18) Malveau, C.; Baille, W. E.; Zhu, X. X.; Ford, W. T. *J. Polym Sci., Part B: Polym Phys.* **2003**, *41*, 2969–2975.
(19) Baille, W. E.; Malveau, C.; Zhu, X. X.; Kim, Y. H.; Ford, W. T. *Macromolecules* **2003**, *36*, 839–847.
(20) Welch, K. T.; Arevalo, S.; Turner, J. F. C.; Gomez, R. *Chem.—Eur. J.* **2005**, *11*, 1217–1227.
(21) Van-Quynh, A.; Filip, D.; Cruz, C.; Sebastiao, P. J.; Ribeiro, A. C.; Rueff, J.-M.; Marcos, M.; Serrano, J. L. *Eur. Phys. J. E* **2005**, *18*, 149–158.
(22) Domenici, V.; Cifelli, M.; Veracini, C. A.; Boiko, N. I.; Agina, E. V.; Shibaev, V. P. *J. Phys. Chem. B* **2008**, *112*, 14718–14728.
(23) Leshchiner, I.; Agina, E.; Boiko, N.; Richardson, R. M.; Edler, K. J.; Shibaev, V. P. *Langmuir* **2008**, *24*, 11082–11088.
(24) Ponomarenko, S. A.; Rebrov, E. A.; Boiko, N. I.; Muzafarov, A. M.; Shibaev, V. P. *Polym. Sci. Ser. A* **1998**, *40*, 763–774; translated from *Visokomolekulyarnye Soedineniya Ser. A* **1998**, *40*, 1253−1265.
(25) Agina, E. V.; Ponomarenko, S. A.; Boiko, N. I.; Rebrov, E. A.; Muzafarov, A. M.; Shibaev, V. P. *Polym. Sci. Ser. A* **2001**, *43*, 1000–1007.
(26) Mijovic, J.; Ristic, S.; Kenny, J. *Macromolecules* **2007**, *40*, 5212–5221.
(27) Anufrieva, E. V.; Krakovyak, M. G.; Anan'eva, T. D.; Vlasov, G. P.; Bayanova, N. V.; Nekrasova, T. N.; Smyslov, R. Yu. *Polym. Sci. Ser. A* **2007**, *49*, 671–677.
(28) Sagidullin, A. I.; Muzafarov, A. M.; Kryakin, M. A.; Ozerin, A. N.; Skirda, V. D.; Ignat'eva, G. M. *Macromolecules* **2002**, *35*, 9472–9479.
(29) Sagidullin, A.; Skirda, V. D.; Tarinova, E. A.; Muzafarov, A. M.; Kryakin, M. A.; Ozerin, A. N.; Fritzinger, B.; Scheler, U. *Appl. Magn. Reson.* **2003**, *25*, 129–156.
(30) Sagidullin, A.; Frirzinger, B.; Scheler, U.; Skirda, V. D. *Polymer* **2004**, *45*, 165–170.
(31) Natali, S.; Mijovic, J. *Macromolecules* **2009**, *42*, 6799–6807.
(32) Hatada, K.; Kitayama, T. *NMR spectroscopy of polymers*; Springer-Verlag: Berlin, 2004.
(33) Pittelkow, M.; Christensen, J. B.; Meijer, E. W. *J. Polym. Sci., Part A: Polym. Chem.* **2004**, *42*, 3792–3799.
(34) Moreno, K. X.; Simanek, E. E. *Macromolecules* **2008**, *41*, 4108–4114.
(35) Rudovsky, J.; Botta, M.; Hermann, P.; Hardcastle, K. I.; Lukes, I.; Aime, S. *Bioconjugate Chem.* **2006**, *17*, 975–987.
(36) Filip, D.; Cruz, C.; Sebastiao, P. J.; Ribeiro, A. C.; Vilfan, M.; Meyer, T.; Kouwer, P. H. J.; Mehl, G. H. *Phys. Rev. E* **2007**, *75*, 011704.
(37) Domenici, V. *Phys. Chem. Chem. Phys.* **2009**, *11*, 8496–8506.
(38) Markelov, D. A.; Gotlib, Yu. Ya.; Darinskii, A. A.; Lyulin, A. V.; Lyulin, S. V. *Polym. Sci. Ser. A* **2009**, *51*, 331–339.
(39) Markelov, D. A.; Lyulin, S. V.; Gotlib, Yu. Ya.; Lyulin, A. V.; Matveev, V. V.; Lahderanta, E.; Darinskii, A. A. *J. Chem. Phys.* **2009**, *130*, 044907.
(40) Karatasos, K.; Adolf, D. B.; Davies, G. R. *J. Chem. Phys.* **2001**, *115*, 5310–5318.
(41) Lyulin, S. V.; Evers, L. J.; van der Schoot, P.; Darinskii, A. A.; Lyulin, A. V.; Michels, M. A. J. *Macromolecules* **2004**, *37*, 3049–3063.
(42) Farrar T. C.; Becker E. D. *Pulse and Fourier Transform NMR Introduction to Theory and Methods*; Academic Press: New York, 1971.
(43) Cai, C.; Chen, Z. Y. *Macromolecules* **1997**, *30*, 5104–5117.
(44) Gotlib, Yu. Ya.; Markelov, D. A. *Polym. Sci. Ser. A* **2002**, *44*, 1341–1350.
(45) Gurtovenko, A. A.; Markelov, D. A.; Gotlib, Yu. Ya.; Blumen, A. *J. Chem. Phys.* **2003**, *119*, 7579–7590.
(46) Gotlib, Yu. Ya.; Markelov, D. A. *Polymer Sci. Ser. A* **2004**, *46*, 815–832.
(47) Gurtovenko, A. A.; Blumen, A. *Adv. Polym. Sci.* **2005**, *182*, 171–282.

(48) Gotlib, Yu. Ya.; Markelov, D. A. *Polymer Sci. Ser. A* **2007**, *49*, 1137–1154.
(49) Francese, G.; Dunand, F. A.; Loosli, C.; Merbach, A. E.; Decurtins, S. *Magn. Reson. Chem.* **2003**, *41*, 81–83.
(50) Lebduskova, P.; Sour, A.; Helm, L.; Toth, E.; Kotek, J.; Lukes, I.; Merbach, A. E. *Dalton Trans.* **2006**, 3399–3406.
(51) Laus, S.; Sour, A.; Ruloff, R.; Toth, E.; Merbach, A. E. *Chem.—Eur. J.* **2005**, *11*, 3064–3076.
(52) Nicolle, G. M.; Toth, E.; Schmitt-Willich, H.; Raduchel, B.; Merbach, A. E. *Chem.—Eur. J.* **2002**, *8*, 1040–1048.
(53) Liu, K.-Z.; Ullman, R. *Macromolecules* **1969**, *2*, 525–528.
(54) Mazo, M. A.; Shamaev, M. Yu.; Balabaev, N. K.; Darinskii, A. A.; Neelov, I. M. *Phys. Chem. Chem. Phys.* **2004**, *6*, 1285–1289.
(55) Kawakami, M.; Byrne, K.; Khatri, B.; McLeish, T. C. B.; Radford, S. E.; Smith, D. A. *Langmuir* **2004**, *20*, 9299–9303.
(56) Khatry, B. S. Ph.D. Thesis, University of Leeds, Great Britain, 2006.
(57) Markelov, D. A.; Neelov, I. M.; Neelov, A. I.; Gotlib; Yu, Ya.; Darinskii, A. A. *Polym. Sci. Ser. A* **2009**, *51*, 940–956.

JP909658V